

# **4× 8 SIW based Slotted Phased Array at Ku Band for Satellite Applications**



By

**Hafsah Niaz Awan**

**MS (EE)-19**

**00000318180**

SUPERVISOR

**Dr. Muhammad Umar Khan**

**DEPARTMENT OF ELECTRICAL ENGINEERING**

A thesis submitted in partial fulfilment of the requirements for the degree

Of Master of Science in Electrical Engineering (MSEE)

at

School of Electrical Engineering and Computer Science (SEECS),

National University of Sciences and Technology (NUST),

Islamabad, Pakistan.

(March 2023)

## **THESIS ACCEPTANCE CERTIFICATE**

Certified that final copy of MS/MPhil thesis entitled "4×8 SIW based slotted phased array at Ku band for satellite applications" written by Hafsah Niaz Awan, (Registration No 318180), of SEecs has been vetted by the undersigned, found complete in all respects as per NUST Statutes/Regulations, is free of plagiarism, errors and mistakes and is accepted as partial fulfillment for award of MS/M Phil degree. It is further certified that necessary amendments as pointed out by GEC members of the scholar have also been incorporated in the said thesis.

Signature: \_\_\_\_\_



Name of Advisor: Dr. Muhammad Umar Khan

Date: 04-Feb-2023

HoD/Associate Dean: \_\_\_\_\_

Date: \_\_\_\_\_


Signature (Dean/Principal): \_\_\_\_\_

Date: \_\_\_\_\_

# Approval

It is certified that the contents and form of the thesis entitled "4×8 SIW based slotted phased array at Ku band for satellite applications " submitted by Hafsah Niaz Awan have been found satisfactory for the requirement of the degree.

Advisor: Dr. Muhammad Umar  
Khan

Signature: 

Date: 04-Feb-2023

---

Committee Member 1: Dr Noshewan Shoaib

Signature: 

13-Feb-2023

Committee Member 2: Dr. Hammad M Cheema

Signature: 

Date:

13-Feb-2023

# Dedication

This thesis is dedicated to my Brother and Husband, who always supported me and fulfilled my dream of higher education. Their effort and struggle have allowed me to have a key to unlocking the mysteries of our world and beyond.

# Certificate of Originality

I hereby declare that this submission titled "4×8 SIW based slotted phased array at Ku band for satellite applications" is my own work. To the best of my knowledge, it contains no materials previously published or written by another person, nor material which to a substantial extent has been accepted for the award of any degree or diploma at NUST SEecs or at any other educational institute, except where due acknowledgement has been made in the thesis. Any contribution made to the research by others, with whom I have worked at NUST SEecs or elsewhere, is explicitly acknowledged in the thesis. I also declare that the intellectual content of this thesis is the product of my own work, except for the assistance from others in the project's design and conception or in style, presentation, and linguistics, which has been acknowledged. I also verified the originality of contents through plagiarism software.

Student Name: Hafsa Niaz Awan

Student Signature:

A rectangular box containing a handwritten signature in blue ink, which appears to read "Hafsa Niaz Awan".

# Acknowledgement

I would like to express my sincere gratitude to Dr. Muhammad Umar Khan for his encouragement and useful critiques and his willingness to give his time so generously.

# Contents

Acknowledgement .....	V
Abstract .....	X
Chapter 1: Introduction .....	1
1.1 Introduction:.....	1
1.2 Satellite Communication:.....	1
1.3 Emerging Technology:.....	3
1.4 Phased Array:.....	3
1.4.1 Fixed Beam Steering: .....	4
1.4.2 Steerable Beam:.....	5
1.5 Research Motivation: .....	6
1.6 Thesis Contribution:.....	7
1.7 Thesis Organization .....	8
Chapter 2: Literature Review .....	9
2.1 Literature Review: .....	9
2.2 Substrate Integrated Waveguide Technology: .....	9
2.3 Current State of Art.....	10
2.4 Research Gap and Thesis Objective: .....	14
Chapter 3: Phased Array Design.....	15
3.1 Substrate Integrated Waveguide: .....	15
3.2 SIW Theory:.....	16
3.3 Design Methodology.....	18
3.4 SIW Antenna Array: .....	20
3.5 SIW Planar 4x8 array:.....	21
3.6 Working Principal:.....	23
3.7 Simulation Results: .....	25
3.8 Block Diagram of Phased Array: .....	28
4.1 Experimental Results: .....	30
4.2 S-Parameters: .....	30
4.3 Radiation Pattern:.....	32
Chapter 5: Conclusion.....	37
5.1 Conclusion .....	37
5.2 Future Work.....	37

References:..... 38



# Figures

Figure 1 Type of Earth orbits [1] .....	1
Figure 2 Rotman Lens [4] .....	4
Figure 3 Beamforming Circuit [4] .....	4
Figure 4 Passive and Active Phased Array [5] .....	5
Figure 5 SIW Structure [21] .....	16
Figure 6 SIW Structure with microstrip geometry [22] .....	17
Figure 7 Via Selection Graph [22] .....	18
Figure 8 SIW Cavity .....	19
Figure 9 SIW Slot antenna .....	20
Figure 10 Linear Slotted array .....	20
Figure 11 Tapered Feed .....	21
Figure 12 4x8 SIW Slot array .....	22
Figure 13 Electric Field Propagation in proposed array .....	23
Figure 14 Surface Current Distribution .....	24
Figure 15 Simulated (S-parameters of antenna, S11 shows the return loss and S21, S31, and S41 shows the mutual coupling between these ports) .....	25
Figure 16 Simulated S-parameters of antenna, S22 shows the return loss and S12, S32, and S42 shows the mutual coupling between these ports. ....	26
Figure 17 Simulated S-parameters of antenna, S33 shows the return loss and S13, S23, and S43 shows the mutual coupling between these ports. ....	26
Figure 18 Simulated S-parameters of antenna, S44 shows the return loss and S14, S24, and S34 shows the mutual coupling between these ports. ....	27
Figure 19 Radiations Pattern .....	28
Figure 20 Block Diagram .....	28
Figure 21 SIW Fabricated Array .....	30
Figure 22 Simulated and measured S-parameters Return loss for Port 1,2,3 & 4 .....	31
Figure 23 Simulated and measured S-parameters of Port 1,2,3 & 4 mutual coupling .....	31
Figure 24 Set up for measurement of far field radiation patterns. ....	32
Figure 25 Beamformer Chip IC Architecture .....	33
Figure 26 0° .....	34
Figure 27:15° .....	34
Figure 28:25° .....	34
Figure 29:35° .....	34
Figure 30:-35° .....	34
Figure 31:-15° .....	34
Figure 32:-25° .....	34

# Tables

Table 1 Comparison Table of State of Art.....	10
Table 2 SIW Antenna Parameters.....	21
Table 3 Comparison with state-of-the-art Phased Array's .....	35

## Abstract

Satellites communications play very important role in global communication nowadays. Applications for communications can be found in several bands, including the L-, X-, Ku-, and Ka-bands. To track satellites Mechanical beam steering is used in conventional agile systems that are commercially available to monitor the satellite. However, these devices are large, expensive to maintain, and have inaccurate mechanical placement. In contrast, Phased array antennas have agile beams, providing significant system advantages and they can track one or more satellites. An important parameter for optimal functioning of satellite-based communication system is the design of its antenna. To meet these requirements aggressive research is underway for low-cost solutions of phased array with larger scanning area. This thesis work also presents substrate integrated waveguide phased array at (14.0-14.5) GHz Ku band for satellite applications., SIW is advantageous for low loss and wide bandwidth due to its high Q-factor, high selectivity, cutoff frequency characteristic, and high-power capacity. The suggested antenna array is built on a single-layer substrate that has a metal ground completely covering it on the back. The SIW operates in the TE<sub>10</sub> mode like a rectangular waveguide filled with dielectric. A 4x8 planar phased array uses the SIW-slot element. It can scan up to  $\pm 35^\circ$  in the whole operating band with maximum measured gain of 19.2dBi and minimum SLL of -10dB.

# Chapter 1: Introduction

## 1.1 Introduction:

This Chapter begins with the brief overview of satellite communication and data traffic growth, followed by multi beam antenna array types to achieve large scanning area. Next it discusses the substrate integrated waveguide potentials for phased arrays. Lastly, it summarizes contribution of this work and organization of this thesis.

## 1.2 Satellite Communication:

Artificial satellites are manmade and launched into different orbits around earth for specific applications. Over a thousand satellites are currently revolving in orbit around the earth. There are different kinds of earth orbit, and each one has benefits and potential. Low earth orbit is at an altitude of 200 to 2,000 km from earth and an orbit takes around 90 minutes to complete. Satellites in medium earth orbit are located at an altitude of 20,000 km, and one orbit takes 12 hours to complete. Geostationary satellites orbit the Earth at a height of 36,000 km. One orbit takes 24 hours to complete. [1]. Following Figure 1 shows the orbits around earth.

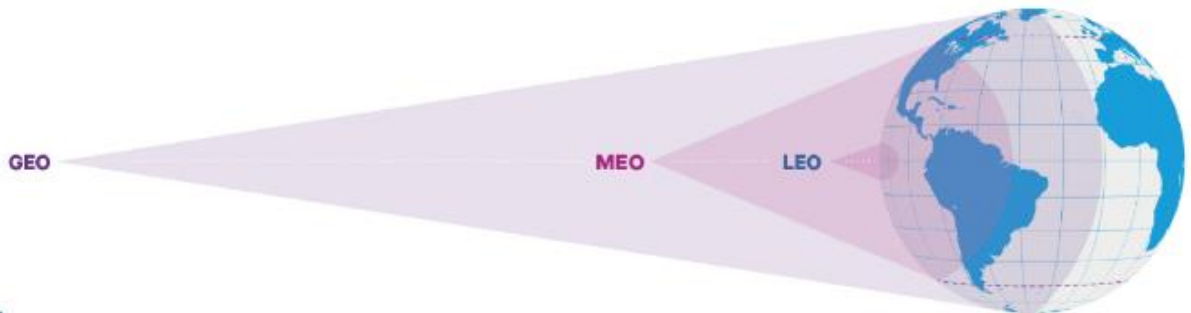


Figure 1 Type of Earth orbits [1]

## **Classes of Orbits:**

### **Geostationary Orbits:**

All radio, television and weather satellites are installed in this orbit. Over the equator, satellites are positioned at a height of around 35,800 kilometers. When viewed from the ground, these geostationary satellites appear to be almost stationary in the sky. Three GEO satellites are present in the orbit that covers almost all parts of the earth. Antennas at baseband can be fixed permanently to send signal. GEO satellites has lifetime of approximately 15 years. [2]

### **Medium Earth Orbit:**

Satellites revolving in this orbit are mostly used for GPS and navigation system. They provide low latency time than GEO satellites and high bandwidth connectivity to service providers, government agencies and commercial enterprises. It brings connectivity to remote areas where laying fiber is not available. Satellites in MEO orbit require high power transmission which also require special type of antennas. [2]

### **Low Earth Orbit:**

LEO satellites have even less latency time than MEO and GEO satellites. Which makes them suitable for emergency situations. Their antennas also can have low transmission power. Almost 3135 satellites are present in LEO orbit for communication purpose. Their plane may be inclined, so they don't always follow the same course around the Earth. LEO offers more alternatives for satellite trajectories, which is one of the reasons it is a popular orbit. Being close to the surface enables it to take photographs with a higher resolution, making it the orbit utilized for satellite imaging the most. Also, because astronauts can fly to and from the International Space Station (ISS) more swiftly and conveniently, it is the orbit in which the ISS is situated. The speed of satellites in this orbit is around 7.8 km/s; at this speed, a satellite completes one orbit of the Earth in about 90 minutes. Communication satellites moves fast across the sky and therefore require smart antenna to track from ground stations. These constellations, which are made up of multiple of the same or related satellites, are occasionally launched together to create a "net" encircling Earth to maximize coverage. Together, they can simultaneously cover a lot of ground on Earth.[2]

### **1.3 Emerging Technology:**

The number of uses for satellite technology is always growing, and satellite technology is evolving quickly. Navigation satellites, gives a GPS receiver's precise location on earth. Cloud imaging, temperature, and precipitation measurements are all done by weather satellites. Communications via the phone, internet, or television are carried out by communication satellites. Earth observation satellites are used to photograph and map the Earth. Typically, frequency bands used for satellite communications are L, S, C and X, Ku, and Ka Band. [3] But as the number of satellites has grown, overcrowding in the lower frequency bands has become a significant problem. To using higher bands, new technologies are being researched. These satellites create a communication path between a transmitter and a receiver positioned throughout the planet. Signals are received by satellites orbiting the earth, which then amplifies and retransmits them using a different frequency. These signals convey information such as voice, audio, video, or any other data. Antennas are employed as the last components of transmitting and receiving systems, allowing communication between the two sides across a distance. These antennas are used to provide fixed or electronically scanned beam as per requirement. [4], Phased array used for electronic beam steering is discussed in the following heading.

### **1.4 Phased Array:**

Due to increase in number of launches, there is also a need of more base stations, so this thesis is aimed to design a multi beam antenna for base station and provide multi beams to track one or more satellites. multiple independent beams can be produced at once by multi-beam antennas from a single aperture. They can be divided into two groups: the passive multi beam antenna and the phased array antenna, depending on how the beams of the multi beam antennas are guided. Basically, there are two types of beams steering fixed and electronically steerable both are discussed below:

### 1.4.1 Fixed Beam Steering:

The antenna system is referred to as a passive multi beam if the complex weight of antenna is set and there are only a few fixed beam patterns. PMB's can be designed using reflector's, lenses or beam forming circuit as shown in Figure 4 and Figure 5.

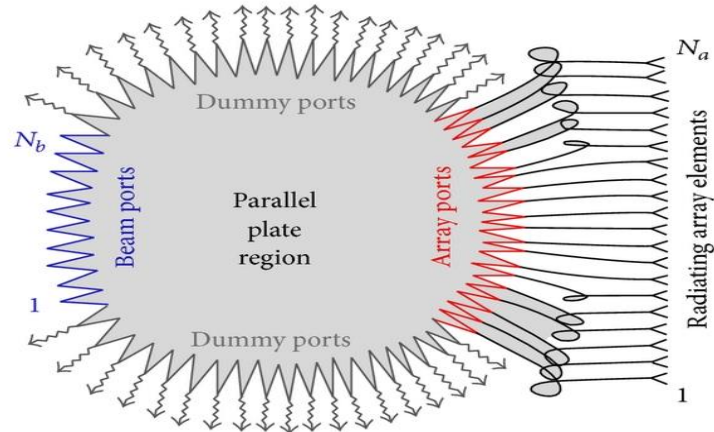


Figure 2 Rotman Lens [4]

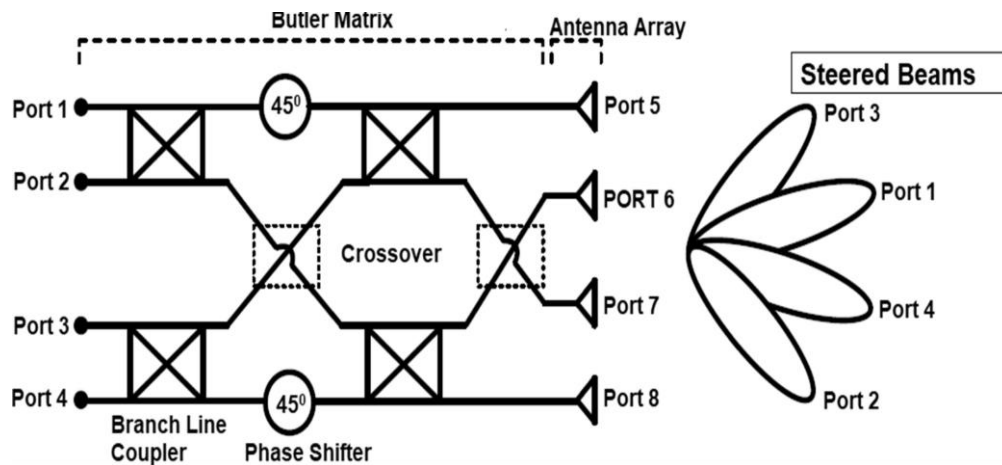


Figure 3 Beamforming Circuit [4]

### 1.4.2 Steerable Beam:

A system is referred to as a phased array antenna if each array element's phase can be adaptively altered and its shaped beam can be constantly guided within a specific angle range.

PAA's can be divided into two main categories:

1. Passive electronically phased array
2. Active electronically phased array

In PAA's each element has its own phase shifter which control's the direction of a wavefront. Active phased array systems shown in Figure 6 needed dedicated radiofrequency (RF) up/down-conversion chain per antenna which is costly and complex. However, in passive phased array we have only one transmitter and receiver. Using PAA's we can scan larger area faster than typical PMBA's, movement of satellite can be tracked in the sky no matter how, or where we move. [5]

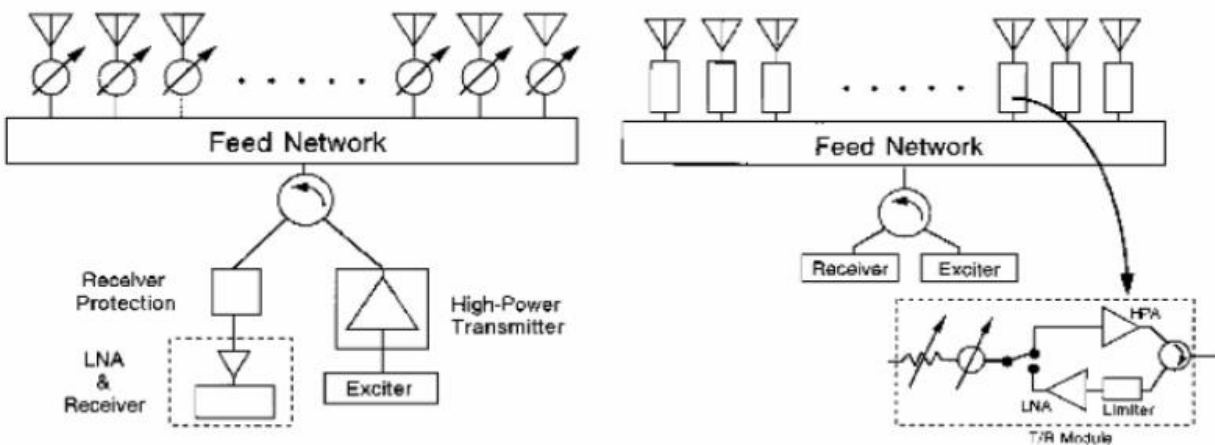


Figure 4 Passive and Active Phased Array [5]

This thesis presents SIW based cheap and compact active antenna array for base station and provide multi beams to track one or more satellites. The phased-array technology's advantage of frequency reuse makes it possible to generate several beams for multiuser or multitarget applications. Analogue RF technique is used in our design because of its reduced power and cost requirement and due to its use of least no. of circuit components. Each array in PAA's is backed



up by a phase shifter, by changing the phase of each phase shifter satellites present in orbit can be tracked.

## **1.5 Research Motivation:**

Today, a rising number of satellites are in orbit around the earth, allowing for a variety of uses in earth observation, communications, navigation, and science. One cannot undervalue how crucial these systems are to our daily lives. The capability of satellites is expanding along with technological development. Due to the rise in recent years of mobile broadband satellite communications. An antenna array with beam scanning capabilities is needed as a crucial part of the mobile terminals in SATCOM On-the-Move (SOTM), which has sparked a lot of research interest. For instance, to ensure coverage, the antenna on Satcom user terminals must typically be able to scan its beam over a wide-angle range. For satellite ground stations, reflector antennas with mechanical steering are typically utilized because of their advantages of high gain and wide operation spectrum. However, they are usually heavy and can only move mechanically to track the satellites, making it impossible for them to communicate with numerous satellites at once. An important piece of equipment for modern satellite communications is the multi beam antenna. By electronically directing the highest radiation towards the desired users while producing nulls against interference sources, it can considerably boost the throughput of wireless communication networks. Star link, a constellation that SpaceX is constructing, has 1,445 satellites in orbit as of April 27, 2021, and is now testing its service in north America, Europe, and New Zealand. 182 LEO satellites have been launched by another satellite broadband provider. There are plans to include additional businesses, some of which are situated in Asia. Kymeta also provides high bandwidth, low profile, and fully integrated phased array for mobile terminals one of their products is kymeta hawk u8 which provides full connectivity solution prepared to offer on-the-go communications and seamless satellite or hybrid satellite/cellular connectivity and attaches conveniently on vehicles and watercraft. [6] The kymeta u8 is depicted in this following Figure 7.



Figure 7 Kymeta u8 Terminal [6]

## 1.6 Thesis Contribution:

SIW Phased array based on cavity-backing technique employing TE<sub>10</sub> mode is presented for Satellite applications. The array is designed by placing 4×8 slots on SIW cavity using TE<sub>10</sub> mode. Cavity-backing technique is employed to make the antenna pattern unidirectional, which is suitable for Satellite communication application. The array exhibits a narrow beam of 26.5° in the E-plane and 16° in the H-plane employing just a single layer structure. Moreover, the antenna array achieves a high gain of 19.8dBi with 94% radiation efficiency. Antenna dimensions are 40×109.2 mm and has a simple microstrip to SIW feed. S-parameters are below -10 dB, which shows that the feed is well matched. Measured and simulated antenna parameters (S-parameters, radiation patterns and other results) are explained in detail in Chapter 4. The results of simulation and measurement are in good agreement.

## **1.7 Thesis Organization**

Rest of the thesis is organized as follows:

1. Chapter 2 covers the extensive literature review on Phased Array's
2. Chapter 3 explains the design procedure in detail which includes the SIW antenna to array design.
3. Chapter 4 includes the detailed analysis of simulation and measurement results.
4. Chapter 5 gives a brief conclusion and future recommendation.

## **Chapter 2: Literature Review**

### **2.1 Literature Review:**

This chapter presents the literature and summarizes the research gaps and presents thesis objective. It also covers a detailed literature review of different phased array's their structure, and characteristics. Wireless technologies, such as SATCOM, 5G, and automobile radar, are moving toward millimeter-wave (mm-W) frequencies to take advantage of the huge accessible frequency range as the demand for faster data rates rises. A phased-array antenna usually provides small size with quick beam scanning as compared to a reflector antenna. These distinguishing characteristics are critical for emerging Ku-band mobile satellite communication, which necessitates a low-profile robust antenna system that can dynamically track the satellite as the terminal moves and maneuvers. Different phased array antennas are also compared to achieve low profile and low-cost array. For that antennas are divided into three different categories.

1. Planar Antennas
2. Single Layer SIW Antennas
3. Multi-layer Antennas

### **2.2 Substrate Integrated Waveguide Technology:**

Planar circuits are cheap and small size. It can be easily combined with integrated circuits but also for their high sensitivity to possible electromagnetic disturbances and their dispersive characteristics in the propagation of the signal. Rectangular waveguides are one of the best solutions to overcome these difficulties[7]. However, with the constant increase in demand for the use of broadband interconnections and compact electronic systems, the latter have seen their interest gradually decrease, due to their cumbersome, very expensive and unsuitable for mass production. Thus, an alternative called substrate integrated waveguides (SIW) technology, which can be employed using printed circuit board (PCB) manufacturing methods[8], [9] and capable of integrating future radio frequency (RF) and ultra-high frequency (UHF) applications [10] is getting a great deal of attention. Since the introduction of SIW to RF systems, many RF

components have been redesigned, including dividers, couplers, diplexers, filters and cavities who previously were developed using microstrips and strip lines [11].

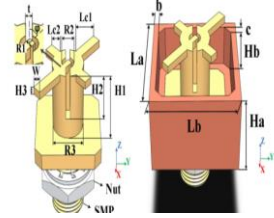
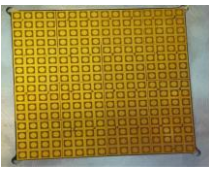
The use of SIW technology, which by its flexibility is one of the most important technologies used for the design of millimeter wave and microwave systems. Indeed, the latter are deployed in a wide field of application, because in addition to having the same advantages as a conventional waveguide, namely a high quality, SIW components have low power consumption, are low cost and easily integrated with the planar circuits. The SIW have also the advantage of being transferable on several types of substrates: PCB, low temperature co-fired ceramic (LTCC) and printing on flexible substrates such as paper or plastic. [12]


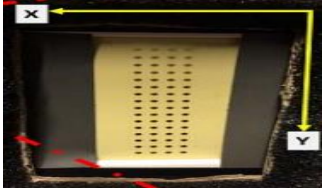
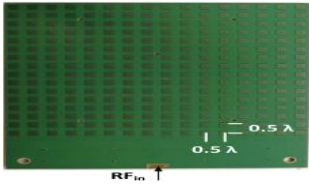

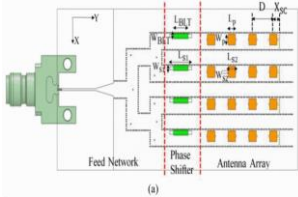

The Table below shows the comparison between different Phased arrays using different antennas for SATCOM applications.

### 2.3 Current State of Art

In recent literature, a variety of Phased arrays designs have been reported, ranging from narrowband to wideband. Study of these designs has been carried out, which includes patch phased arrays, dipole antenna phased arrays, antenna, with increased efficiency and [13 to 20].

Table 1 Comparison Table of State of Art

Paper	Figure	Frequency (GHz)	No. of elements/ Gain	Coverage	Antenna Type	Phase Shifter	Comments
AWPL 2021 [13]		13.1-14.5	16x16 28.3dBi	$\pm 40^\circ$ x-z plane and y-z plane)	Cross Dipole with metal Cavity Antenna	IC used against each element	Complex Antenna structure with metal cavity, no phase shifter reduction
IMS 2019 [14]		30 GHz TX 20GHz RX	16x16/ 28.8dBi	$\pm 70^\circ$ x-y plane	Multi-Layer Aperture coupled antenna	Beamformers IC used each having 8 outputs	Multi-Layer Antenna, no phase shifter reduction, each 8 element uses 1 beamformer IC

TAP 2019 [15]		29.5-30	1×4 / 7.4dBi	$\pm 38^\circ$ in x-y plane	Aperture Patch Antenna	Magnetic Actuator	No, phase shifter IC used, low gain, complex antenna design
TAP [2019] [16]		29.5-30 GHz	4×16/ 15.5dBi	$\pm 40^\circ$ In y-z	Multi-Layer Aperture coupled antenna	8 Beamformer IC used each having 8 outputs	Low gain, complex antenna structure and no phase reduction, not cost effective
TAP [2020] [17]		14 GHz	16×16/ 29dBi	$40^\circ$ x - z $15^\circ$ x - y	Patch Antenna	Phase Shifter	Approx $\approx 70$ Phase shifter ICs are used for 256 elements, less scanning range
TAP [2015] [18]		Receiver (12.25– 12.75) GHz Transmitter 14.0–14.5 GHz	4×16/ 35dBi	$15^\circ$ – $75^\circ$ x-y $0$ – $360^\circ$ x-z	Rectangular Waveguide	6-Bit phase shifter IC using against each element	Complex and expensive Antenna Design, no phase shifter reduction
IMS 2020 [19]		29–31 GHz	1×4 8.2dBi	$\pm 20^\circ$ in x-z	SIW Rectangular waveguide	Tunable Transmission Type with High dielectric Slab	Low Gain, less scanning range and no phase shifter IC used
AWPL 2021 [20]		14.4-16.8	4× 16 / 7.4dBi	$60^\circ$ in x-z $60^\circ$ in x-y	Stacked Patch Substrate Integrated Waveguide	Phase shifter against each element	2 substrates are used, with no phase shifter reduction

In Ref [13] A circularly polarized phased array with  $16 \times 16$  Ku-bands is suggested. A cross dipole, a metal chamber, and a threaded SMP connection make up the antenna element. The metal cavity increases the antenna's gain while decreasing mutual coupling between array members, providing good return loss and axial ratio for 2D scanning. When the cavity is added,

the center element's mutual coupling at center frequency is -26.6 dB. Phased array has Return Loss of -10 dB at a scanning angle of 40° in the xz and yz planes (13.1-14.5 GHz). The major lobe's Axial Ratio is less than 2 dB over the entire scanning range. Gain fluctuation is also less than 3dB.

In Ref [14] a new modular design for active phased array with a broad steering angle for K/Ka-band mobile Satellite communication systems is suggested. Active phased-array design is less complicated and expensive when using the suggested modular approach. It provides a 16-module, 256-element (16X16) A-PAA (4X4 construction pieces). The suggested phased array has S<sub>11</sub> < -10 and a scanning range of 40° in the xz and yz planes with a mutual coupling of -26.6 dB for the center element at center frequency (13.1-14.5 GHz).

In Ref [15] offers a low-profile, high-performance, and cheap (PAA) system for the Ka-band. investigated, created, and tested a 1 x 4 passive subarray operating in the Ka-band frequency spectrum as a potential part of satellite communication systems. It is demonstrated and thoroughly experimentally proven that a better outcome passive phase shifter is used with a CP antenna. To accurately regulate the phase state of the phase shifter, magnetic actuator is presented. With a measured radiation efficiency of 60% throughout the frequency band, the proposed CP passive PAA produces right-hand CP radiation with good cross-polarization discrimination over a wide scan angle range of 0° to 38°. (29.5-30.5 GHz).

Ref [16] shows the implementation of CP Active Phased array operating at Ka Band. Array is composed of sixty-four antennae arranged in rectangular grid. Eight Beamformer ICs with eight RF output channels were used to manipulate the complex weight and magnitude across the antenna aperture. Antenna array has three metal layers and constructed utilizing inexpensive printed circuit board (PCB) technology for a modular and scalable Ka -band PAA with a large looking angle. The measured radiation pattern shows a (RHCP) pattern with an axial-ratio Axial Ratio level of 3 dB and a small pointing inaccuracy of 1.5° throughout a scanning angular range of 0° to 40°.

In Ref [17] Outlines various methods for decreasing the quantity of phase shifters in a 2-D phased array while having a certain scan range in the x-y and y-z planes by decreasing sidelobes below a set threshold. By controlling random groupings of components, grating lobes are suppressed and fewer phase shifters are required. 16x16 phased array at 14 GHz were tested to

check the performance of randomly partitioned phased arrays. It is shown that by adjusting random groupings of components, grating lobes are suppressed and fewer phase shifters can be used. It also provides advice for choosing the best method of randomly dividing a phased array into subgroups. 75% decrease in phase shifters is possible while maintaining an x-y scan range of  $40^\circ$ , a y-z scan range of  $15^\circ$ , and sidelobes of -10 to -12 dB both with and without a 6 dB taper.

In Ref [18] waveguide hybrid phased array for Ku-band mobile satellite communications has been described in research. The small size and inexpensive array uses an electrical scan in elevation and a mechanical scan in azimuth to monitor targets. An electrical scan in elevation and a mechanical scan in azimuth are used by the unobtrusive and low-cost array to keep an eye on satellites. The array architecture is divided into 12x225 mm tall inclined and interlaced subarrays. Duplexers and feed networks are constructed using odd waveguide diameters. The system consists of 12 distinct transmitter and receivers' modules with phased shifter elements for beam and polarization tracking. By electronically scanning 15 to 75 degrees in elevation and physically scanning 360 degrees in azimuth, the device is designed to track satellites. The maximum gain loss in the scanning range is 4.0 dB.

Ref [19] discusses a high gain, passive, SIW, Ka-band 4x4 PAA. Four SIW phase shifters for the beamforming network make up the SIW-based PAA, which also includes a series fed network to boost gain. In simulations scanning range of  $-30^\circ$  to  $+30^\circ$  is achieved for the whole working band of 29-31 GHz. The maximum simulated gain is 15.2 dBi at 30 GHz.

Ref [20] An element and array of wideband substrate integrated waveguide (SIW) cavity-backed antennas are constructed. Physically linked stacked patches are used to construct the SIW cavity-backed array element. The two patch radiators are directly connected to the coaxial pin. It makes the array more expensive and complex. The proposed element has Return Loss  $<10$  dB at (14.5–17.4 GHz). Array has a maximum gain of 7.4dBi and can scan up to  $80^\circ$  in the H-plane at (14.4–15.6 GHz).



## 2.4 Research Gap and Thesis Objective:

The Papers mentioned in Table [2.1] are different patch and waveguide arrays using phase shifters for each element in array to achieve larger scanning area which increases expenditure and complications of phased array. They are also using phase shifters for each element which increases the overall cost of array. Only paper [9] shows the SIW antenna but it has low gain and less scanning range. Maximum scanning achieved using 70 phase shifters for 256 elements having scanning range of  $40^\circ$  in azimuth and  $15^\circ$  in elevation. So, we need an array which uses less no of phase shifters and have simple design.

Therefore, this thesis focuses on:

- Designing SIW based antenna with cavity backed approach to suppress back lobe and achieve high gain with less losses
- Designing of  $4 \times 8$  Planar SIW slotted array to achieve the directivity and scanning range of  $\pm 35^\circ$
- Designing Planar array in such a way to achieve maximum scanning range with limited no of phase shifter.

## Chapter 3: Phased Array Design

In this chapter, the design of SIW antenna is explained in detail. It focuses on designing cavity backed SIW antenna based on TE<sub>10</sub> mode with narrow beam and high gain. First designing of SIW line is described in Section 3.1. In Section 3.2, Next antenna design based on TE<sub>10</sub> mode is explained and analyzed. Based on the results obtained from it, 32 elements antenna array is designed and discussed in Section 3.3. In the last Section 3.4, the parametric analysis of the antenna is explained.

### 3.1 Substrate Integrated Waveguide:

SIW are the well-known planar implementation of conventional rectangular waveguides. The two copper layers of planar printed circuit board (PCB) acts as upper and lower walls of metallic waveguide while the side walls of conventional waveguide are realized by metallic circular Vias in the PCB (Fig. 5). SIW provides all the benefits of conventional rectangular waveguides with thin form factor at the same time. Features of SIW include high quality factor, low leakage losses, high power handling, and non-susceptibility to cross talk. Because of these features a planar antenna system at higher frequencies can be realized without any compromise on efficiency irrespective of substrate's dielectric constant. The geometry of SIW structure is shown in Figure 6. The metal cylinders or vias of the sidewalls are placed with controlled periodicity to support the propagation of guided waves with minimal radiation loss [21]. SIW provides the benefit of lower loss in comparison to Microstrip/Strip line counterparts with minimal penalty in size and cost. To design SIW waveguide, different formulae have been derived in literature for calculating the spacing between the parallel vias wall (represented by 'a' in Fig. 6). However, in this thesis formula of [5] is used to calculate the Width of SIW cavity using via spacing and diameter.

Additionally, it also offers in-plane transitions to microstrip and GCPW easing the connections with other microwave components on the same substrate. Planar transitions microstrip to SIW is used for feeding mechanism.

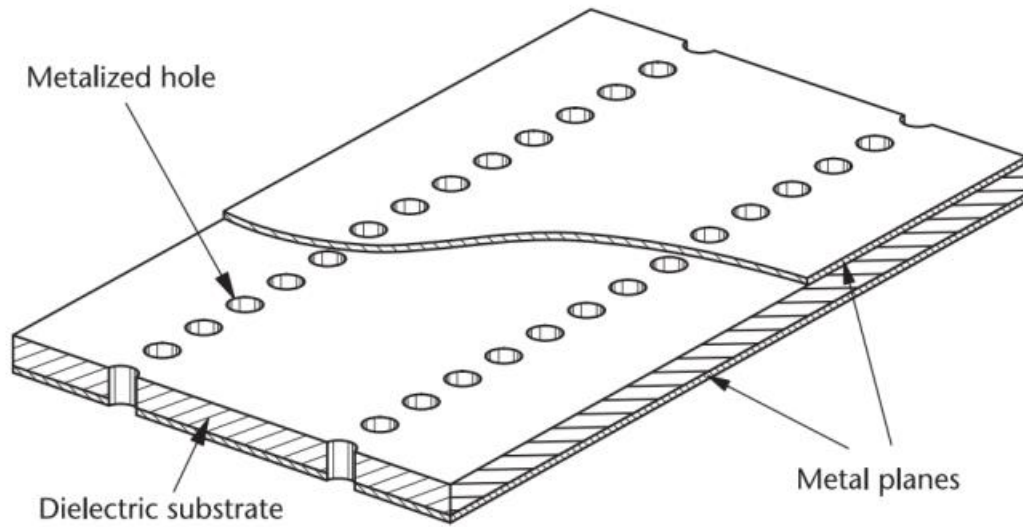


Figure 5 SIW Structure [21]

### 3.2 SIW Theory:

The substrate integrated waveguide is formed by two conductive planes, separated by a dielectric substrate, with sidewalls each consisting of a row of metalized cylinders spaced with a certain periodicity.

Designing procedure of Substrate Integrated Waveguide and Feeding Technique is mentioned below

The cutoff frequency for air filled rectangular waveguide is given by [22]

Equation 1

$$f_{c_{mn}} = \frac{c}{2\pi\sqrt{\epsilon_r}} \sqrt{\left(\frac{m\pi}{W}\right)^2 + \left(\frac{n\pi}{h}\right)^2}$$

For TE<sub>10</sub> mode

Equation 2

$$fc = \frac{c}{2W}$$

Where “W” is the longer dimension of equivalent rectangular waveguide.

With air filled rectangular waveguide

Equation 3

$$W = \frac{c}{2fc}$$

Width of the dielectric filled rectangular waveguide is given by.

$$Wd = \frac{W}{\sqrt{\epsilon_r}}$$

Equation 4

For SIW, two parameters are important, the via diameter “d” and the distance between the vias “s” as shown in Figure 3-1, which is given by [22]

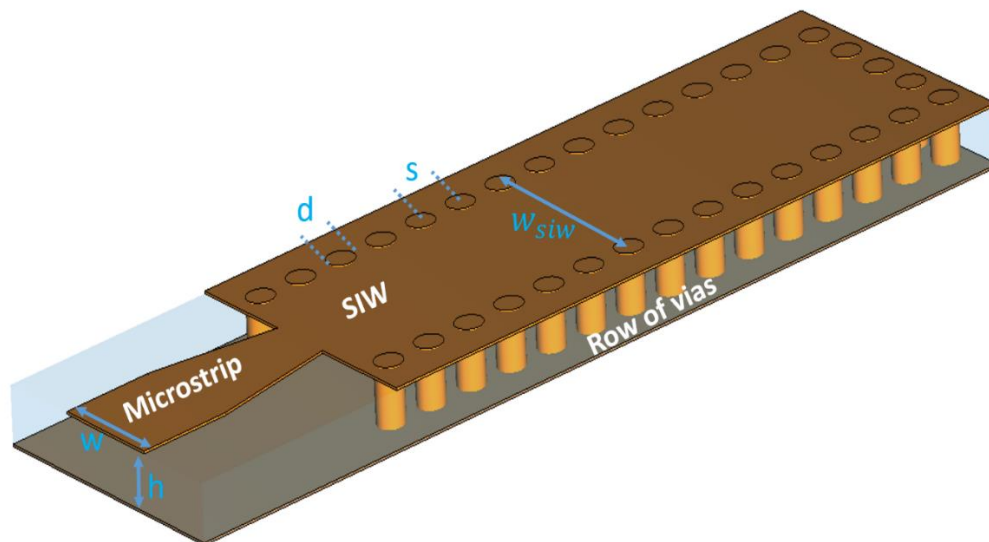


Figure 6 SIW Structure with microstrip geometry [22]

To find the width of SIW we can use the following formula,

Equation 5

$$W_{SIW} = Wd - \frac{d^2}{0.95 \times s}$$

Equation 6

$$d < \frac{\lambda g}{5} \text{ and } s < 2d$$

The above equations limits are graphically represented in Fig 9. When the via's diameter is greater than the spacing between two consecutive vias, the design of SIW become realizable but on the other hand if it is chosen below lower limit, there will be leakage through vias.

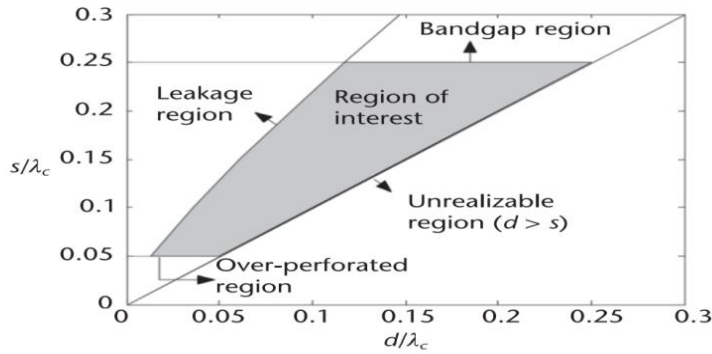


Figure 7 Via Selection Graph [22]

### 3.3 Design Methodology

#### SIW Cavity:

First SIW cavity was designed for desired TE<sub>10</sub> mode using equation [2, 6]. Design of Single Cavity is shown Figure 8. Figure 8 shows the structure of SIW cavity on a RT Duroid 5880 substrate ( $\epsilon_r=2.2$  and loss tangent is 0.009) with a thickness of 1.575 mm. The substrate integrated waveguide is formed by two conductive planes, separated by a dielectric substrate, with sidewalls each consisting of metalized via holes with the diameter ‘ $d$ ’ and the distance between vias ‘ $s$ ’.

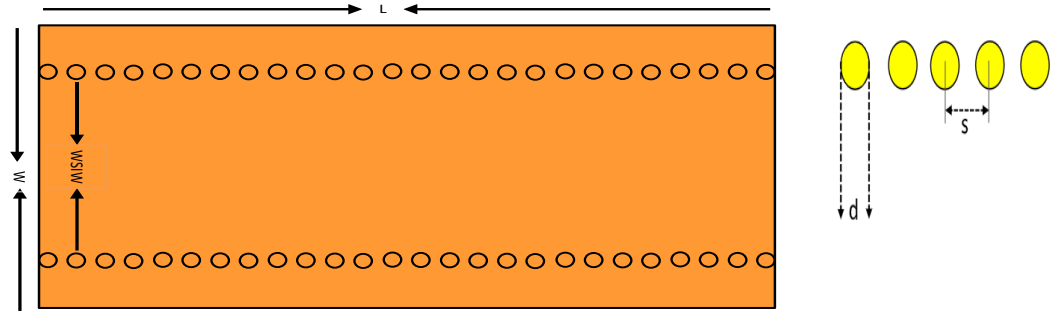


Figure 8 SIW Cavity

### SIW Slot Antenna:

Next an and a radiation slot, on the top right was added. Slot has been added in SIW line for radiation at (14.0 to 14.5) GHz. The slots width and length has been calculated according to the following equation:

$$\text{Slot Length} = \frac{\lambda_0}{\sqrt{2(\epsilon_r + 1)}} \quad \text{Equation 7}$$

$$\text{Slot Width} < \frac{\text{Slot Length}}{2} \quad \text{Equation 8}$$

Slot is placed in such a way to get maximum radiation and good S11. One end of the cavity was also shorted by adding vias to make it a standing wave antenna. At this point the antennas results were analyzed, and parametric study was performed to achieve resonance and optimum performance at (14-14.5) GHz. Figure 9 shows the structure. The size of single antenna is  $19 \times 35.84 \text{ mm}$ .

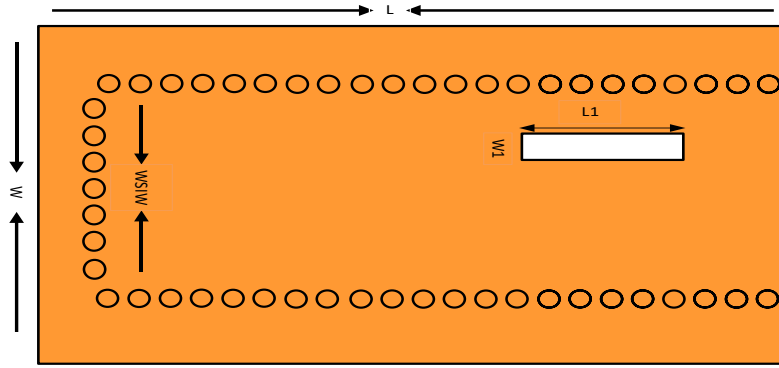


Figure 9 SIW Slot antenna

### 3.4 SIW Antenna Array:

To achieve high directivity seven more slots were added with center-to-center slot distance is considered as  $\frac{\lambda_g}{2}$  to increase the directivity. Slot position was chosen at higher current densities to achieve high radiations. Figure 10 shows the SIW  $1 \times 8$  slotted array.

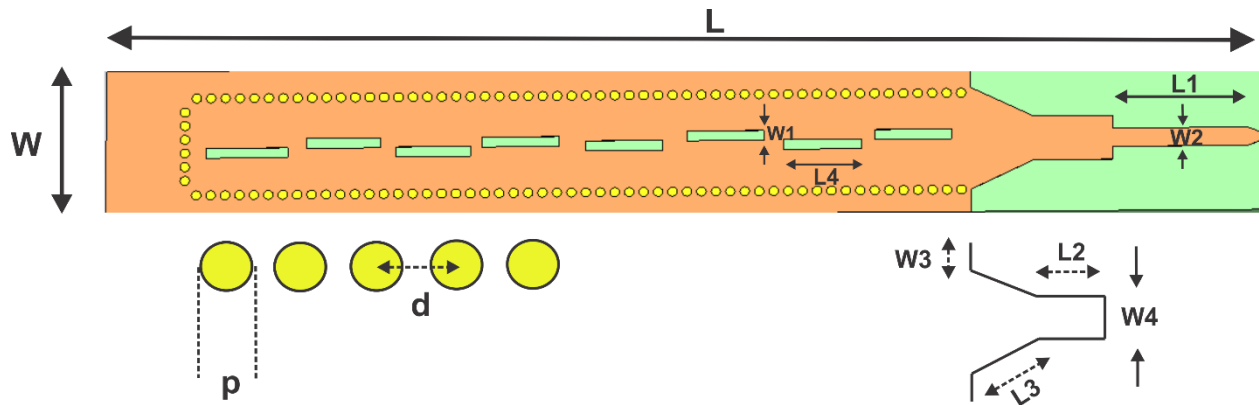


Figure 10 Linear Slotted array

To feed the array Microstrip to SIW transition is used in which Taper length is chosen as a multiple of a quarter of wavelength to minimize the return loss and are chosen according to criteria given below:

$$\frac{\lambda_g}{2} < L5 < \lambda_g \quad \text{Equation 9}$$

$$W5 = 0.4 \times Ag \quad \text{Equation 10}$$

Where “Ag” is a waveguide width. [24]. Dimensions of SIW line particular transition has been chosen because of its easy optimization. The dimensional view of the microstrip to SIW transition is shown in Figure 11 and, all these design parameters are tabulated in Table 2.

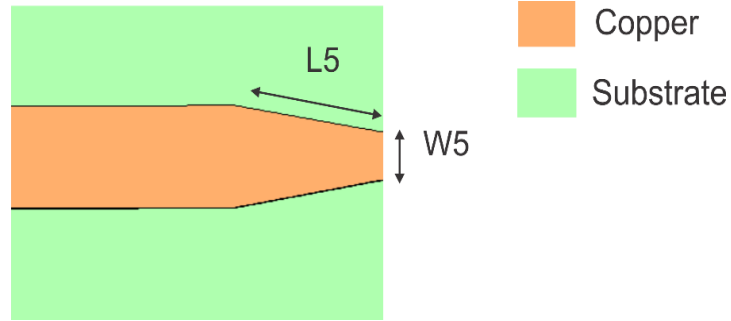


Figure 11 Tapered Feed

Table 2 SIW Antenna Parameters

Parameter	Value (mm)	Parameter	Value (mm)
L	109.01	W	16
L1	14.03	W1	1.08
L2	8.21	W2	2.00
L3	7.23	W3	1.4
L4	8.00	W4	4.80
L5	1.48	W5	0.98
d	1.50	p	1.00

### 3.5 SIW Planar 4x8 array:

Implementation of active phased array for the proposed SIW structure as shown in Figure 12, 4x8 SIW based slotted waveguide antenna array is designed with dimension of  $W_b= 40.01\text{mm}$  and  $L_a=109.01\text{mm}$  shown in Figure 12. The interelement spacing is  $\frac{\lambda}{2}$  to avoid grating lobes.



Phase shifting at the input terminal is directly supplied into simulations with the aid of the simulator.

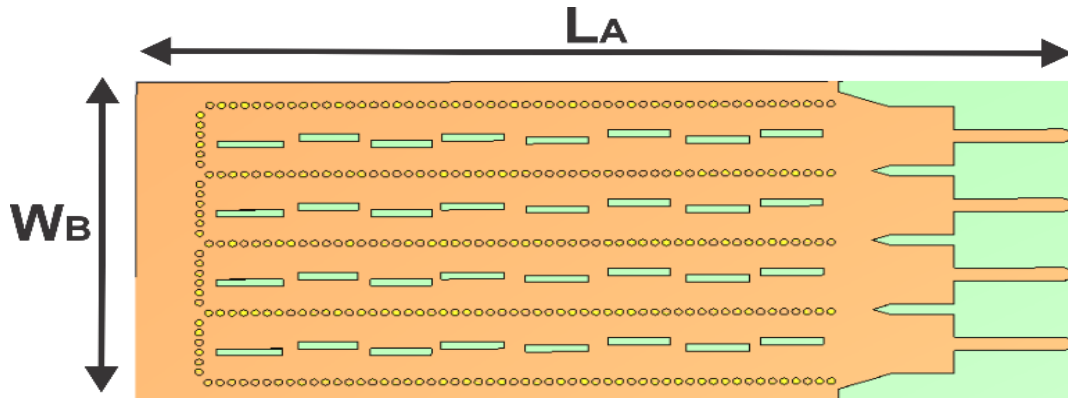


Figure 12 4x8 SIW Slot array

Array scans from broadside towards end-fire direction by changing phase at input terminal with maximum gain of 19.8dBi. To steer the beam of above shown figure electronically, we give different progressive phase shifts at each port to analyze beam shifting at desired direction. Following equation is used to find the progressive phase shift.

$$\beta = -kdsin\theta \quad \text{Equation 11}$$

Where “ $\theta$ ” is the looking angle and “ $d$ ” is the interelement spacing between antenna elements.

### 3.6 Working Principal:

The antenna is designed in TE<sub>10</sub> mode because it has least cut off frequency, TM modes are not supported in substrate integrated waveguides, because there is a continuous surface current along the direction of side walls, since it does not have side walls it has discrete walls. Spacing of vias is designed in such a way to avoid leakage. Figure 13 shows the simulated structure of the SIW cavity. It shows the electric field distribution for the TE<sub>10</sub> mode at 14.25 GHz inside the SIW cavity. The analysis has been performed in CST Studio. Since there is no transverse magnetic component in SIW, Transverse electric field around slots is taking part in radiation.

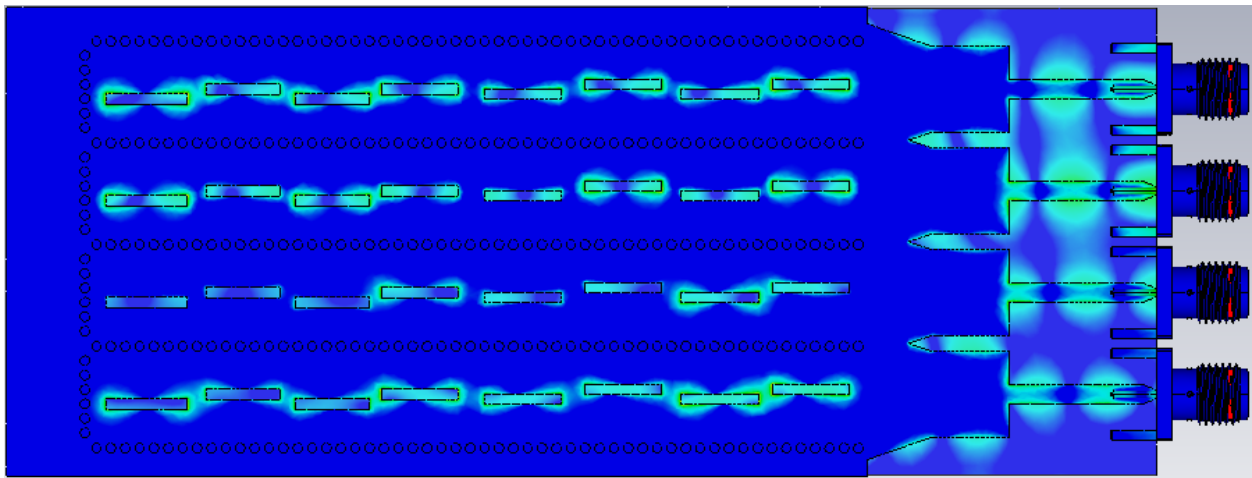


Figure 13 Electric Field Propagation in proposed array

It is desirable that the operating frequency of the radiating structure should be at 14.25 GHz; hence, SIW is designed for lower cutoff frequency of 9.375GHz.

Surface current distribution has been studied at center frequency to explore the resonance characteristics of the antenna as shown in Figure 14. SIW is working in TE<sub>10</sub> mode, the slot exhibits longitudinal ( $y$ -axis) and transverse ( $x$ -axis) current components as shown in Figure 14. Due to the current movement in opposite direction, there is a 180-degree phase shift at  $\frac{\lambda_g}{2}$  spacing so the slots are placed at alternate positions to have same phase and same amplitude.

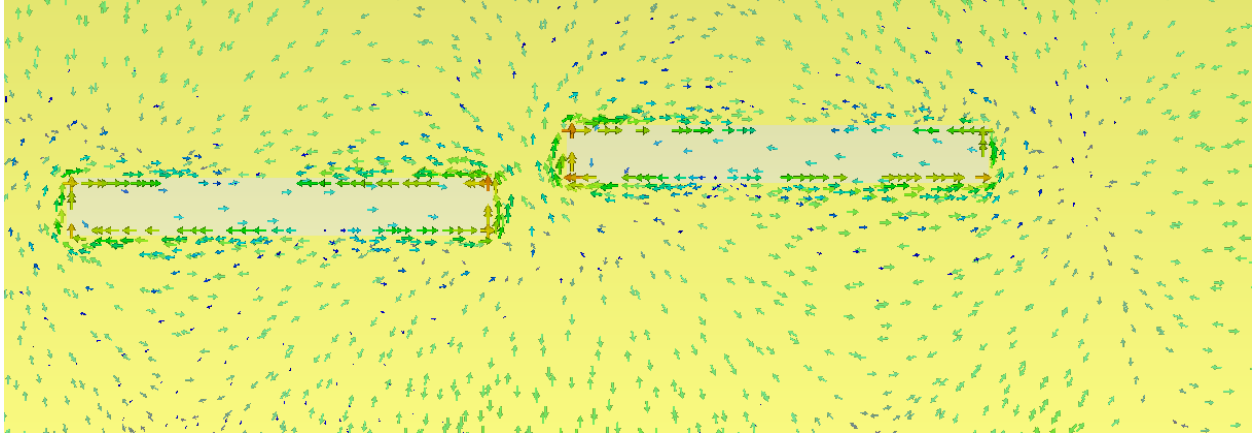


Figure 14 Surface Current Distribution

SIW to microstrip transition has been employed for feeding the antenna. The structure consists of tapered line act as bridge between the SIW and the  $50 \Omega$  microstrip line. The transition used in from microstrip to SIW is based on principle of same dielectric substrate. The taper is used for converting the microstrip line quasi-TEM mode into SIW TE<sub>10</sub> mode. Because the substrate is same, electric field orientation of both structures are approximately in same direction.

### 3.7 Simulation Results:

The proposed antenna is simulated and optimized in CST Studio. The 35 $\mu$ m copper thickness is used in both simulation and fabrication. The antenna achieves a considerable bandwidth ( $|S_{11}| < -10$  dB) of 0.5GHz (14GHz-14.5GHz). The simulated S-parameters and cross talk between all ports are shown in Fig. 15 to 18. Antenna has also a simulated radiation efficiency greater than 94%.

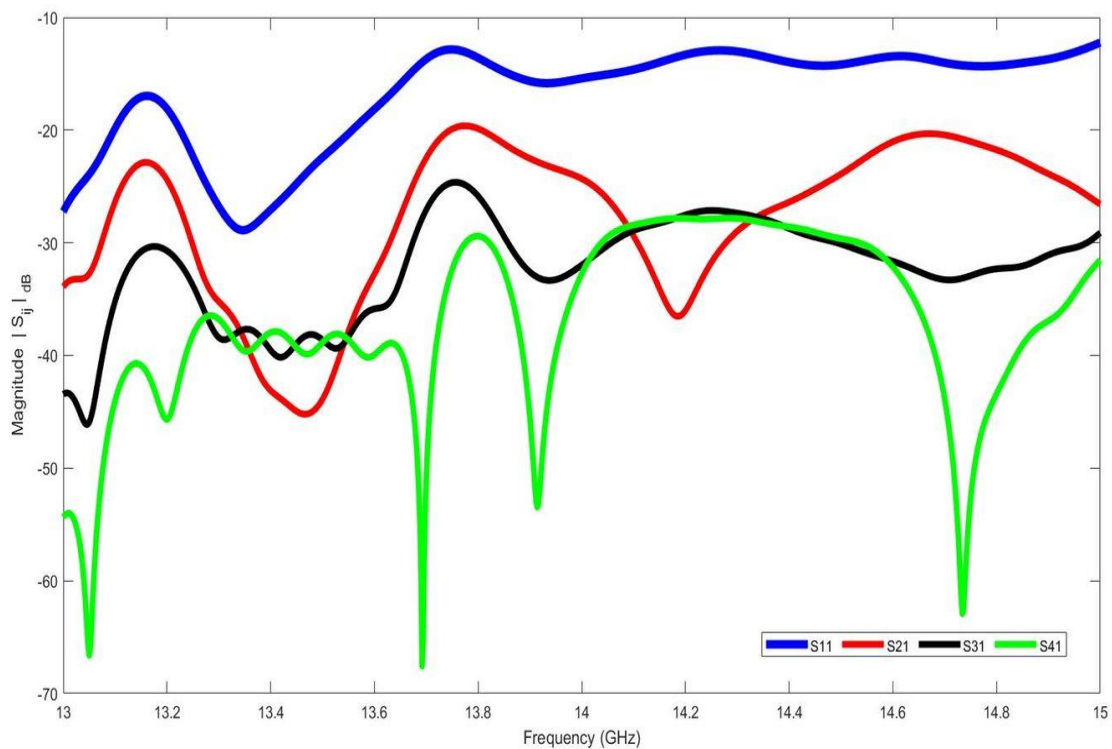


Figure 15 Simulated (S-parameters of antenna, S11 shows the return loss and S21, S31, and S41 shows the mutual coupling between these ports)

In the above Figure it can be seen  $S_{11} < -10$  dB for (14-14.5) GHz band. And mutual coupling of all ports with port 1 is also less than -20dB.

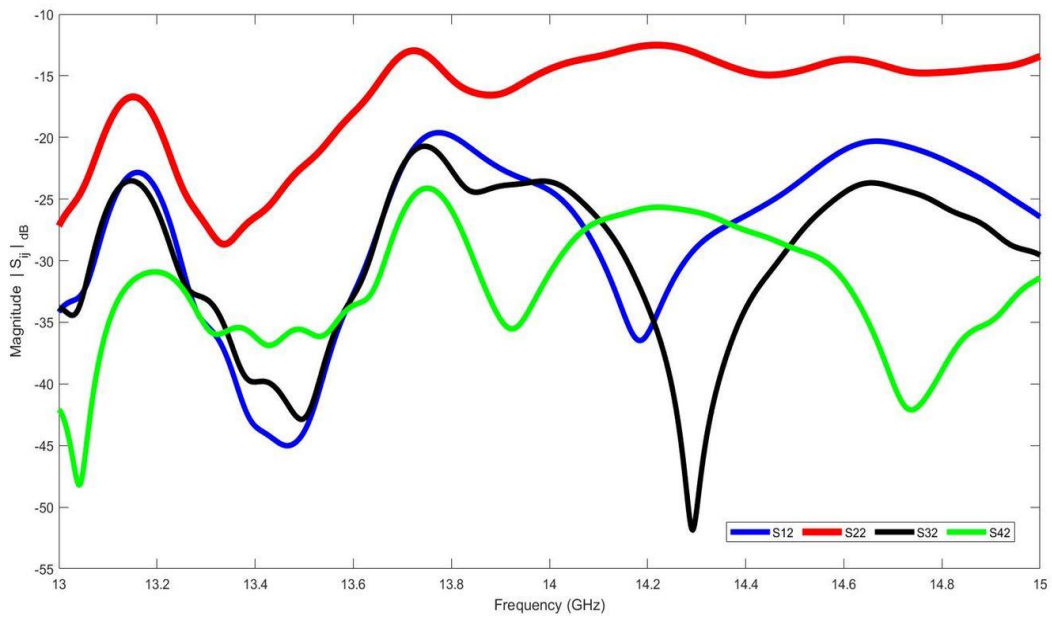


Figure 16 Simulated S-parameters of antenna, S22 shows the return loss and S12, S32, and S42 shows the mutual coupling between these ports.

In the above Figure it can be seen  $S_{22} < -10$  dB for (14-14.5) GHz band. And mutual coupling of all ports with port 2 is also less than -20dB.

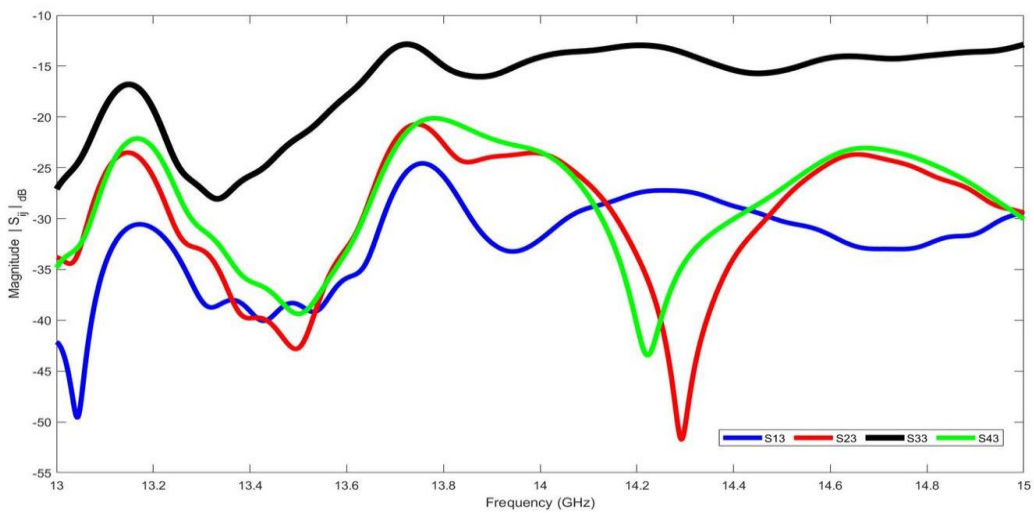


Figure 17 Simulated S-parameters of antenna, S33 shows the return loss and S13, S23, and S43 shows the mutual coupling between these ports.

In the above Figure it can be seen  $S_{33} < -10$  dB for (14-14.5) GHz band. And mutual coupling of all ports with port 3 is also less than -20dB.

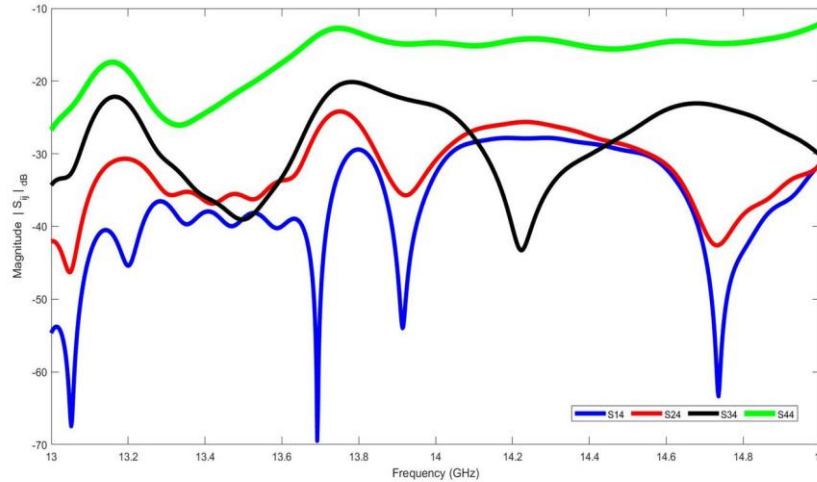


Figure 18 Simulated S-parameters of antenna, S44 shows the return loss and S14, S24, and S34 shows the mutual coupling between these ports.

In the above Figure it can be seen  $S_{44} < -10$  dB for (14-14.5) GHz band. And mutual coupling of all ports with port 4 is also less than -20dB.

Array shown in Figure 12 is fed with 4 sets of progressive phase shifts according to equation [11] to achieve beam shifting in desired direction as shown in Figure 18. The simulated Gain for broadside direction at three different frequencies is 19.8dB, 19.2dB and 19dB respectively. Beamwidth at  $0^\circ$  are observed as 25.7deg, 25.5deg and 25.2deg respectively. The scanning range in phi-90 is from  $-35^\circ$  to  $35^\circ$ . 1D Polar plots at different titled beams are shown in Figure 19.

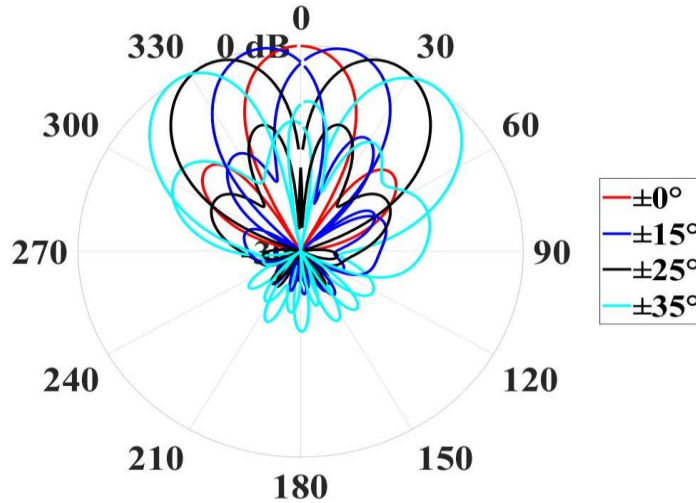


Figure 19 Radiations Pattern

In above Figure Beam scanning is analyzed there is a  $1^\circ$  Gain Variation as we move from  $0^\circ$  to  $35^\circ$  and beam widens due to limited spacing between the elements and mutual coupling effect. The maximum gain achieved at broadside is  $19.8^\circ$

### 3.8 Block Diagram of Phased Array:

To analyze the beam in different angle Progressive Phase Shifts were given in simulation, For Practical purpose ADAR1000 will be integrated with antenna. ADAR1000 will be used to control the beams of phased array by giving progressive phase using Phase Shifters. Block diagram of Integrated Circuit is in Figure [20]

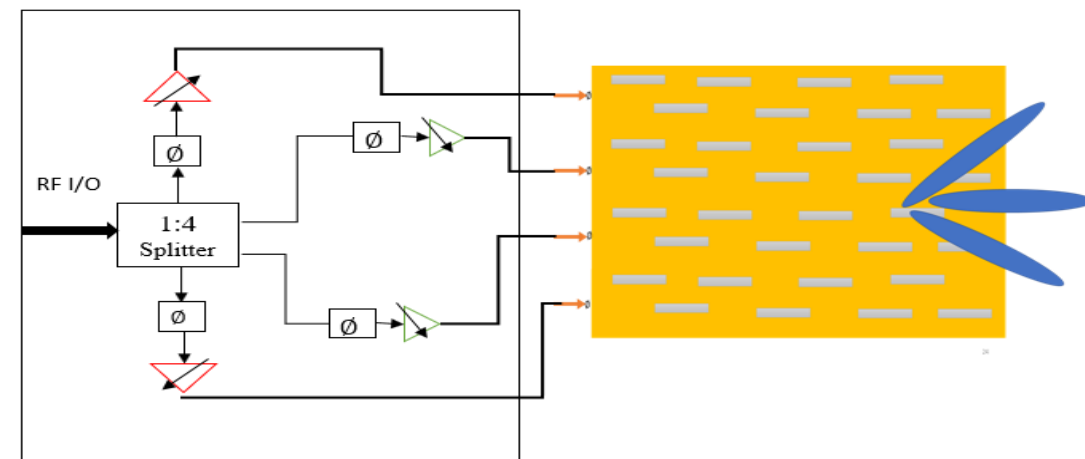


Figure 20 Block Diagram

In Active Phased array, a full control of amplitude and phase is required. Beamformer IC is used to regulate the elements phase and amplitude. Each receiver channel features an LNA, followed by a phase shifter and a driver amplifier, as seen in the above image. It offers a full 360° Phase adjustment range in the RF Path with a 6 bit phase resolution, in addition to a 31dB gain adjustment range. The registers will be controlled using a straightforward 4 wire SPI control. In this scenario, the receiver will receive input, after which each path will accept the input, apply the phase shifts, and then combine once more at the RF I/O pin to allow for the analysis of the beam patterns.



## Chapter 4: Experimental Results

### 4.1 Experimental Results:

As mentioned in the last chapter, the antenna is implemented on rogers duroid5880, the fabricated prototype of the antenna is shown in Figure 21. This chapter covers the measurement results, which verifies the concept of the proposed Phased array. Results will also be compared with the simulated Results.

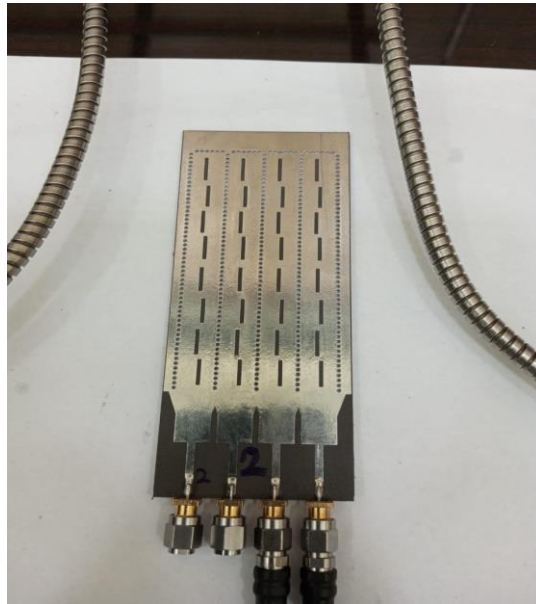


Figure 21 SIW Fabricated Array

### 4.2 S-Parameters:

Both simulated and measured scattering parameters of the presented antenna array are compared in Figure 22 and 23 showing good agreement with each other. Vector network analyzer (VNA) is employed for measurement of  $S_{11}$  of the antenna. Since the VNA has two port and antenna has four ports, the S-parameters were measured in following manner: two port of antenna was kept 50 ohms terminated and S-parameters were measured for rest of the two ports. This process was repeated two times to get return losses and mutual coupling of all ports. It can be seen from Figure 20 and 21 that  $S_{11}$  is below -10 dB from 14 GHz to 14.5 GHz, which confirms the effectiveness of the microstrip feed design. Although both simulated and measured  $S_{11}$  are below

-10 dB, but the latter has slightly less bandwidth and a slight frequency shift due to fabrication error and the SMA connector.

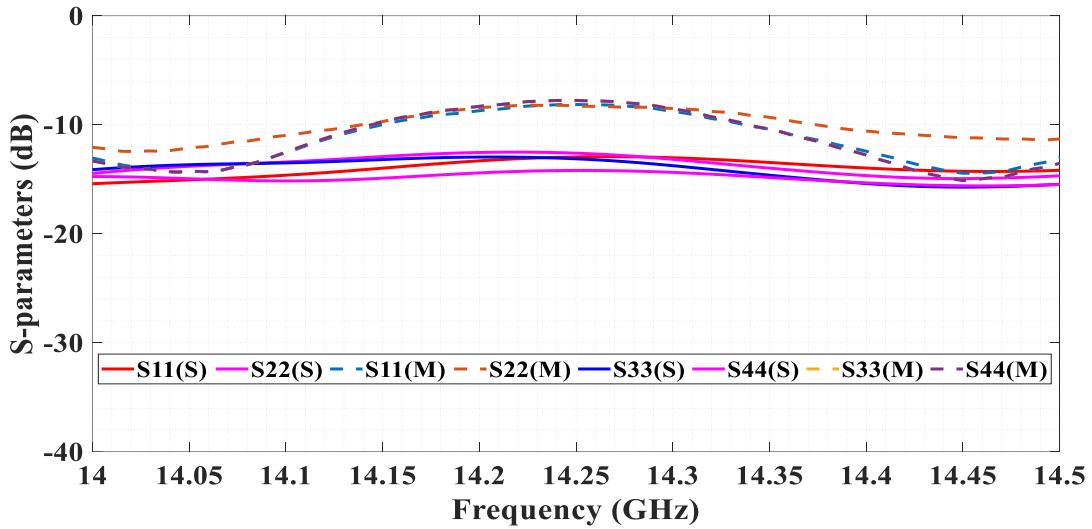


Figure 22 Simulated and measured S-parameters Return loss for Port1,2,3 & 4

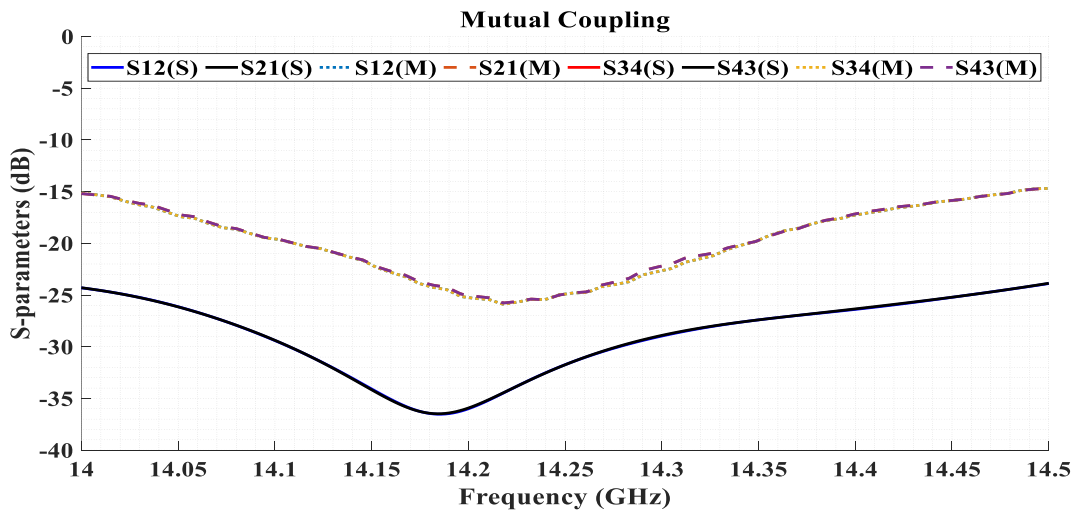


Figure 23 Simulated and measured S-parameters of Port 1,2,3 & 4 mutual coupling

### 4.3 Radiation Pattern:

In a far-field anechoic chamber, radiation patterns are measured, and Figure 24 depicts the measurement setup. Antenna radiates effectively into space in the range of 14 GHz to 14.5 GHz. Maximum measured gain for the antenna is 19.2dBi.

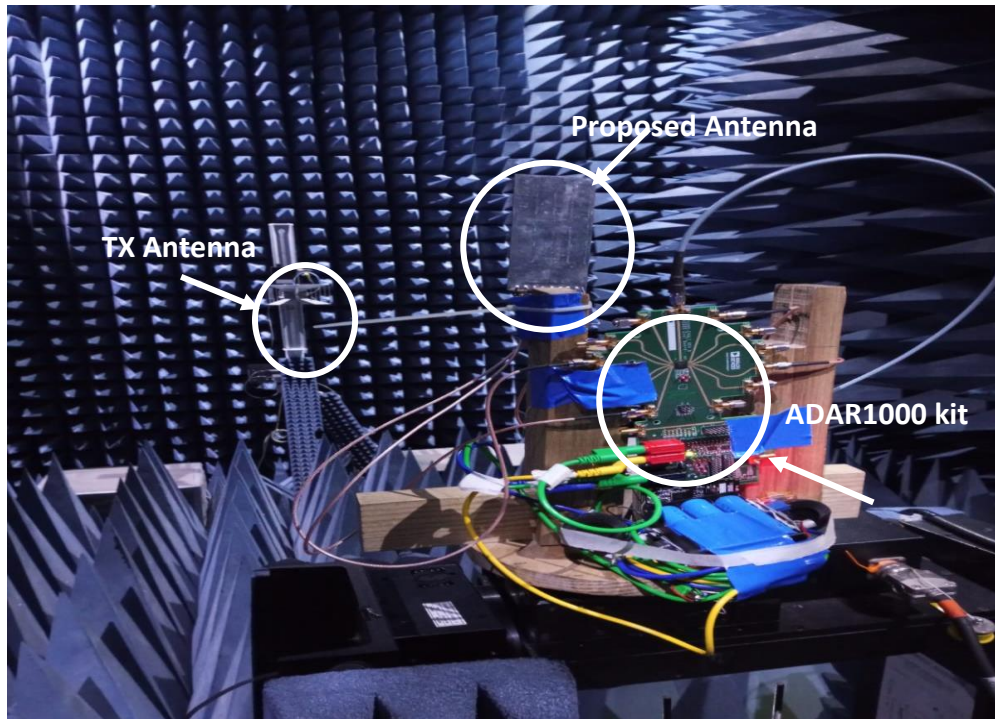


Figure 24 Set up for measurement of far field radiation patterns.

Beamformer chip IC shown in Figure 25 is integrated with Antenna array to observe radiation patterns at different angles. It is four channel beamformer IC and each channel has its own transmitter and receiver chain containing power amplifiers, attenuators, and phase shifters for X and Ku frequency bands. [25] Transmitter chain is used to feed each antenna port with different progressive phase shifts and beam was at different angles.

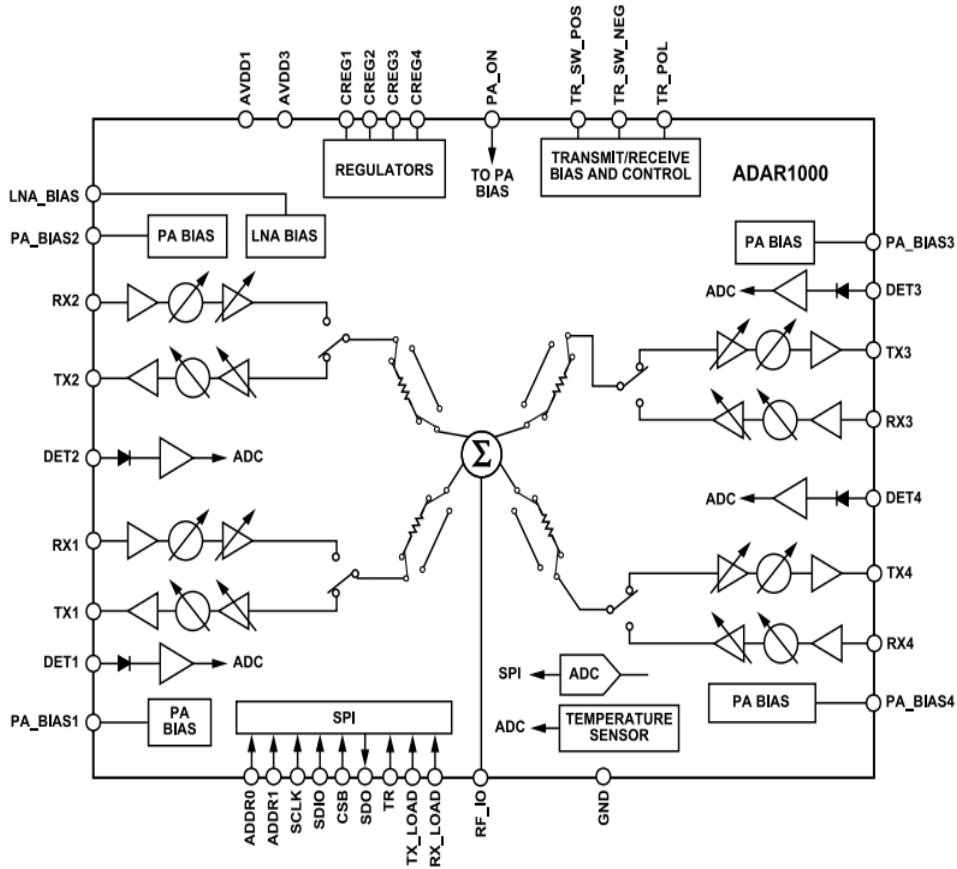


Figure 25 Beamformer Chip IC Architecture

A simulated radiation efficiency of 94% is achieved. This high value is due to utilization of cavity and avoiding feed network losses because of simple feed structure.

Figures 26 to 32 show the antenna's normalised measured and simulated radiation patterns at a frequency of 14GHz. The results from simulations and measurements are very similar. The fabrication tolerances are thought to be the cause of a slight decrease in the measured results. The measured scanning range is between  $-35^\circ$  and  $+35^\circ$ , which deviates somewhat from the anticipated scanning angle of between  $-40^\circ$  and  $+40^\circ$ .

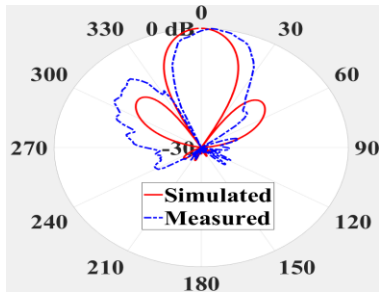


Figure 26 : 0°

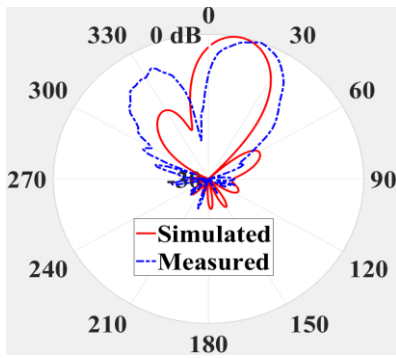


Figure 27:15°

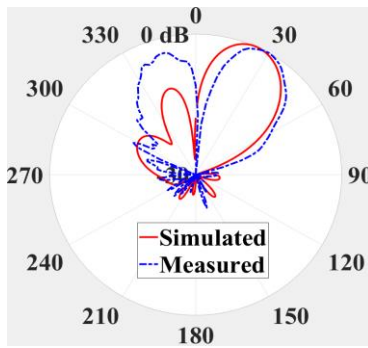


Figure 28:25°

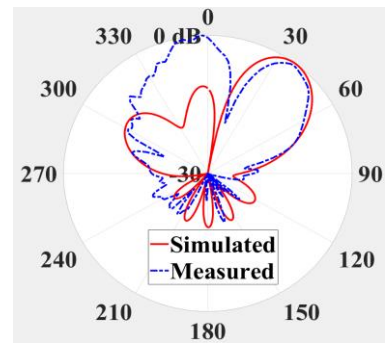


Figure 29:35°

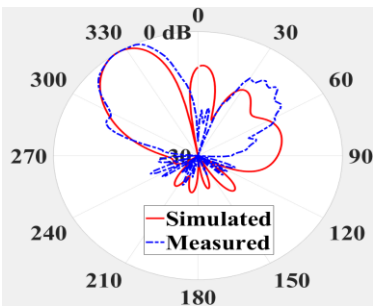


Figure 30:-35°

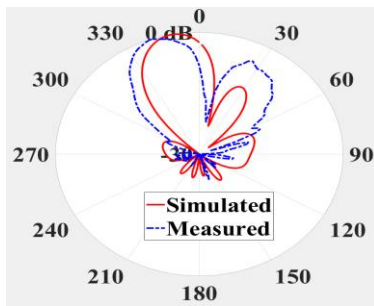


Figure 31:-15°

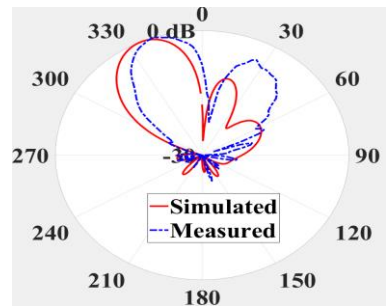


Figure 32:-25°

A little discrepancy between the results from simulation and measurement is observed, which may be the result of measuring equipment flaws like the phase inaccuracy brought on by cables, adapters, and alignment concerns. Within the scanning range, the gain fluctuations are less than 2dB. The computed results and the measured sidelobe level at 14GHz in the E-plane are in good agreement. The antenna has a measured beamwidth of 26.5 degrees in the E-plane, which is in line with the predictions made by simulations. Table 3 displays a comparison of the given antenna with current technology.

Table 3 Comparison with state-of-the-art Phased Array's

<b>Sr. No</b>	<b>Frequency GHz</b>	<b>Gain dBi</b>	<b>No. of elements</b>	<b>Coverage Degrees</b>	<b>Antenna Type</b>	<b>No. of Phase shifter</b>
[26]	13.1 to 14.5	28dBi	256	+/-40° x-z plane	Cross Dipole with metal Cavity	256
[27]	29.5-30	15.5dBi	64	+/-40° x-z plane	Multi-Layer Aperture coupled antenna.	64
[28]	29-31	7.9	4	+/-20 ° x-z plane	SIW slotted antenna	Tunable transmission line
[29]	14.4-16.8	7.4	64	60 ° x-z plane 60° x-y plane	Stacked Patch SIW cavity	64
<b>This Work</b>	<b>14-14.5</b>	<b>19.0</b>	<b>32</b>	<b>+/-35 ° x-z plane</b>	<b>SIW slotted antenna</b>	<b>4</b>

In Ref [26] A circularly polarized phased array with 16 ×16 Ku-bands is designed with scanning range of 40° in the xz and yz planes, the proposed array achieves Return Loss<-10 dB at (13.1-14.5 GHz). Each element uses its own phase shifter which increased the overall cost of array.

In Ref [27] describes the implementation of CP Active Phased array operating at Ka Band. Array is composed of 64 elements arranged in rectangular grid. Antenna is designed in three metal layers which makes antenna design complex. Throughout a scanning range of 0° to 40°, with

maximum gain of 15.5dBi, phase shifter reduction was not employed, and each element uses its own phase shifter IC which.

In Ref [28] discusses a passive phased array antenna with a 7.9dBi for the Ka-band that is a 4x4 substrate integrated waveguide (SIW). Four SIW phase shifters for the integrated with PAA make up the SIW-based PAA, which also includes a SIW-series fed network to increase gain. In simulations -30° to +30° scanning range is achieved at 29-31 GHz.

In Ref [29] An element and array of wideband (SIW) cavity-backed antennas are constructed. Physically linked stacked patches are uses two patch radiators are directly connected to the coaxial pin. It makes the array more expensive and complex. The proposed element has  $S_{11} < 10$  dB at (14.5–17.4 GHz). According to simulation results, the infinite array has a maximum gain of 7.4dBi and can scan up to 80° in the H-plane with bandwidth (14.4–15.6 GHz).

The proposed work is composed of SIW cavity backed slotted phased array. The SIW phased array is built in a single layer. Which attains maximum measured gain of 19.2dBi at broadside and achieved a scanning range of  $\pm 35^\circ$ . With minimum SLL of -10dB for maximum scanning range.

## **Chapter 5: Conclusion**

### **5.1 Conclusion**

In this thesis, a low-cost, high gain with  $\pm 35^\circ$  scanning range slotted antenna based on substrate integrated waveguide (SIW) is presented. Dominant mode (TE<sub>10</sub>) inside the SIW is excited by employing a simple SIW to microstrip transition feed. The array of  $4 \times 8$  slotted antennas are employed to make the cavity radiate. The proposed prototype is designed, fabricated, and experimentally verified in an anechoic chamber. The antenna exhibits a narrow beam of  $26.5^\circ$  in the E-plane. In addition, the antenna achieves a measured gain of 19.2dBi with 94% radiation efficiency. Measured and simulated results are in close agreement with each other. This antenna is considered a potential candidate Ku band satellite application.

### **5.2 Future Work**

As future extension, more work can be done to narrow the beam by further using more radiating elements. Instead of a simple SIW, half mode SIW can be employed for miniaturization. The antenna can be designed at high frequencies, which will further reduce the size. Dual Band array can be designed to use same phased array for uplink and downlink channels. Array can be made reconfigurable to operate at different channels at a same time.



## References:

1. H. Naito and S. Yamamoto, "Is better access to mobile networks associated with increased mobile money adoption? evidence from the micro-data of six developing countries," *Telecommunications Policy*, vol. 46, no. 6, p. 102314, 2022.
2. "Types of orbits," ESA. [Online]. Available: [https://www.esa.int/Enabling\\_Support/Space\\_Transportation/Types\\_of\\_orbits](https://www.esa.int/Enabling_Support/Space_Transportation/Types_of_orbits). [Accessed: 08-Mar-2023].
3. Q. Luo and S. Gao, "Smart antennas for satellite communications on the move," 2017 International Workshop on Antenna Technology: Small Antennas, Innovative Structures, and Applications (iWAT), Athens, Greece, 2017, pp. 260-263, doi: 10.1109/IWAT.2017.7915374.
4. H. Al-Saedi et al., "A Low-Cost Ka-Band Circularly Polarized Passive Phased-Array Antenna for Mobile Satellite Applications," in *IEEE Transactions on Antennas and Propagation*, vol. 67, no. 1, pp. 221-231, Jan. 2019, doi: 10.1109/TAP.2018.2878335.
5. W. Hong et al., "Multibeam Antenna Technologies for 5G Wireless Communications," in *IEEE Transactions on Antennas and Propagation*, vol. 65, no. 12, pp. 6231-6249, Dec. 2017, doi: 10.1109/TAP.2017.2712819.
6. "Hawk U8," Kymeta Corp, 20-Jul-2022. [Online]. Available: <https://www.kymetacorp.com/solutions/hawk-u8/>. [Accessed: 08-Mar-2023].
7. J. B. Lee, S. H. Lee, K. W. Lee, J. Kim, C. G. Kim, and Y. J. Yoon, "A New type of the matching structure of a H-plane T-junction for a high-power system," 2010 IEEE Int. Symp. Antennas Propag. CNC-Usn. Radio Sci. Meet. - Lead. Wave AP-SURSI 2010, 2010, doi: 10.1109/APS.2010.5561941.
8. Scheiner et al., "Microstrip-to-waveguide transition in planar form using a substrate integrated waveguide," *IEEE Radio Wirel. Symp. RWS*, vol. 2018-January, pp. 18–20, Feb. 2018, doi: 10.1109/RWS.2018.8304934.

9. B. Wang and Y. J. Cheng, "Broadband Printed-Circuit-Board Characterization Using Multimode Substrate-Integrated-Waveguide Resonator," *IEEE Trans. Microw. Theory Tech.*, vol. 65, no. 6, pp. 2145–2152, Jun. 2017, doi: 10.1109/TMTT.2017.2650232.
10. W. Hong, K. H. Baek, and S. Ko, "Millimeter-Wave 5G Antennas for Smartphones: Overview and Experimental Demonstration," *IEEE Trans. Antennas Propag.*, vol. 65, no. 12, pp. 6250–6261, Dec. 2017, doi: 10.1109/TAP.2017.2740963
11. Sahu, V. K. Devabhaktuni, R. K. Mishra, and P. H. Aaen, "Recent advances in theory and applications of substrate-integrated waveguides: A review," *Int. J. RF Microw. Compute. -Aided Eng.*, vol. 26, no. 2, pp. 129–145, Feb. 2016, doi: 10.1002/MMCE.20946.
12. S. G. Mallick, G. A. Kumar, S. Chatterjee, B. Biswas, and D. R. Poddar, "Transitions from SIW to various transmission lines for substrate integrated circuits," 2019 URSI Asia-Pac. Radio Sci. Conf. AP-RASC 2019, Mar. 2019, doi: 10.23919/URSIAP-RASC.2019.8738245.
13. L. -K. Zhang, Y. -X. Wang, J. -Y. Li, Y. Feng and W. Zhang, "Cavity-Backed Circularly Polarized Cross-Dipole Phased Arrays," in *IEEE Antennas and Wireless Propagation Letters*, vol. 20, no. 9, pp. 1656-1660, Sept. 2021, doi: 10.1109/LAWP.2021.3092148
14. W. M. Abdel-Wahab et al., "A Modular Architecture for Wide Scan Angle Phased Array Antenna for K/Ka Mobile SATCOM," 2019 IEEE MTT-S International Microwave Symposium (IMS), 2019, pp. 1076-1079, doi: 10.1109/MWSYM.2019.8700842.
15. H. Al-Saedi et al., "A Low-Cost Ka-Band Circularly Polarized Passive Phased-Array Antenna for Mobile Satellite Applications," in *IEEE Transactions on Antennas and Propagation*, vol. 67, no. 1, pp. 221-231, Jan. 2019, doi: 10.1109/TAP.2018.2878335.
16. H. Al-Saedi et al., "An Integrated Circularly Polarized Transmitter Active Phased-Array Antenna for Emerging Ka-Band Satellite Mobile Terminals," in *IEEE Transactions on Antennas and Propagation*, vol. 67, no. 8, pp. 5344-5352, Aug. 2019, doi: 10.1109/TAP.2019.2913745.
17. B. Rupakula, A. H. Aljuhani and G. M. Rebeiz, "Limited Scan-Angle Phased Arrays Using Randomly Grouped Subarrays and Reduced Number of Phase

- Shifters," in *IEEE Transactions on Antennas and Propagation*, vol. 68, no. 1, pp. 70-80, Jan. 2020, doi: 10.1109/TAP.2019.2935100.
18. G. Han, B. Du, W. Wu and B. Yang, "A Novel Hybrid Phased Array Antenna for Satellite Communication on-the-Move in Ku-band," in *IEEE Transactions on Antennas and Propagation*, vol. 63, no. 4, pp. 1375-1383, April 2015, doi: 10.1109/TAP.2015.2389951.
  19. Z. R. Omam, W. M. Abdel-Wahab, S. Gigoyan and S. Safavi-Naeini, "High Gain  $4 \times 4$  SIW Passive Phased Array Antenna," 2020 IEEE International Symposium on Antennas and Propagation and North American Radio Science Meeting, 2020, pp. 45-46, doi: 10.1109/IEEECONF35879.2020.9329752.
  20. H. Liu, A. Qing, Z. Xu, Z. Yu and S. Zhang, "Design of Physically Connected Wideband SIW Cavity-Backed Patch Antenna for Wide-Angle Scanning Phased Arrays," in *IEEE Antennas and Wireless Propagation Letters*, vol. 20, no. 3, pp. 406-410, March 2021, doi: 10.1109/LAWP.2021.3053413.
  21. M. S. Majedi and A. R. Attari, "Design and analysis of new substrate integrated waveguide resonance antennas," 6th International Symposium on Telecommunications (IST), Tehran, Iran, 2012, pp. 24-28, doi: 10.1109/ISTEL.2012.6482947.
  22. Substrate integrated waveguide (no date) *Microwaves101*. Available at: <https://www.microwaves101.com/encyclopedias/substrate-integrated-waveguide> (Accessed: December 15, 2022).
  23. B. Kunooru, S. V. Nandigama, D. Ramakrishna, R. Gugulothu, and S. Bhalke, "Studies on microstrip to SIW transition at Ka-band," Proc. 2019 TEQIP - III Spons. Int. Conf. Microw. Integr. Circuits Photonics Wirel. Netw. IMICPW 2019, pp. 379–382, May 2019, doi: 10.1109/IMICPW.2019.8933234.
  24. Moitra, Sourav et al. "Ku-band Substrate Integrated Waveguide (SIW) Slot Array Antenna for Next Generation Networks." *Global journal of computer science and technology* 13 (2013)
  25. "RF Wireless World," Microstrip to SIW transition | SIW to Microstrip Transition. [Online]. Available: <https://www.rfwireless-world.com/Terminology/Microstrip-to-SIW-Transition.html>. [Accessed: 08-Mar-2023].

26. ADAR1000 (2018) Datasheet and Product Info | Analog Devices. Available at: <https://www.analog.com/en/products/adar1000.html#product-reference> (Accessed: December 15, 2022).
27. L. -K. Zhang, Y. -X. Wang, J. -Y. Li, Y. Feng and W. Zhang, "Cavity-Backed Circularly Polarized Cross-Dipole Phased Arrays," in *IEEE Antennas and Wireless Propagation Letters*, vol. 20, no. 9, pp. 1656-1660, Sept. 2021, doi: 10.1109/LAWP.2021.3092148
28. H. Al-Saedi et al., "An Integrated Circularly Polarized Transmitter Active Phased-Array Antenna for Emerging Ka-Band Satellite Mobile Terminals," in *IEEE Transactions on Antennas and Propagation*, vol. 67, no. 8, pp. 5344-5352, Aug. 2019, doi: 10.1109/TAP.2019.2913745.
29. Z. R. Omam, W. M. Abdel-Wahab, S. Gigoyan and S. Safavi-Naeini, "High Gain  $4 \times 4$  SIW Passive Phased Array Antenna," 2020 IEEE International Symposium on Antennas and Propagation and North American Radio Science Meeting, 2020, pp. 45-46, doi: 10.1109/IEEECONF35879.2020.9329752.
30. H. Liu, A. Qing, Z. Xu, Z. Yu and S. Zhang, "Design of Physically Connected Wideband SIW Cavity-Backed Patch Antenna for Wide-Angle Scanning Phased Arrays," in *IEEE Antennas and Wireless Propagation Letters*, vol. 20, no. 3, pp. 406-410, March 2021, doi: 10.1109/LAWP.2021.3053413.